

Analyzing Airline Alliances through Multi-Attribute Graph Partitioning to Maximize Competition and Market Penetration Capability

Khalil Al Handawi^{a,*}, Fabian Bastin^b

^a*McGill University, Department of Mechanical Engineering, Macdonald-Stewart Building, 817 Sherbrooke W, Montreal, QC, Canada H3A 2T7*

^b*University of Montreal, Department of Computer Science And Operations Research, CP 6128 Succ Centre-Ville, Montreal, QC, Canada H3C 3J7*

Abstract

The air transportation market is highly competitive and dynamic. Airlines often form alliances to expand their network reach, improve operational efficiency, and enhance customer experience. However, the impact of these alliances on market competition and operational efficiency is not fully understood. In this paper, we propose a novel approach to analyze airline alliances using multi-attribute graph partitioning. We develop metrics to quantify the competitiveness of flight segments and the market penetration capability of airlines based on their alliance memberships. We formulate a bi-objective optimization problem to maximize both competition and market penetration simultaneously. We also propose algorithms to solve this optimization problem and demonstrate their effectiveness using real-world flight schedule data. Our results provide insights into the structure of airline alliances and their implications for market competition and operational efficiency.

Keywords: Airline alliances, Graph partitioning, Competition index, Market penetration capability, bi-objective optimization

1. Introduction

Air transportation involves complex logistics and specifics for transporting passengers around the globe. Airlines commonly *interline* with competitors to allow their passengers to switch airlines along routes. This practice allows airlines to offer more destinations and expand their network. Airlines tend to collaborate closely on specific routes and aspects of air transportation to provide an attractive “joint” product to passengers that goes beyond interlining. This cooperation is often formalized in the form of:

- **Alliances:** where airlines cooperate on a broader scale, and on offering reciprocal benefits to passengers.
- **Antitrust immunity:** where airlines are allowed to cooperate on pricing and scheduling without violating antitrust laws.
- **Codesharing agreements:** where airlines share the same physical flight but are able to independently sell tickets under their own brand.
- **Joint ventures:** where airlines cooperate on a specific route or set of routes by sharing revenue, costs, and coordinating schedules.

Airline alliances and other forms of cooperation also benefit passengers in terms of lower interline fares by internalizing the costs to the airlines. The airlines simultaneously benefit from the increased passenger volumes and the ability to offer a more comprehensive network to passengers (Brueckner and Whalen, 2000). However, as soon as consolidation decreases competition, passengers may lose depending on the market power effect (Bilotkach and Hüschelrath, 2019). While airline alliances are thought to enhance network efficiency and market reach, the actual impacts can be complex and varied. The evidence suggests that not all alliances lead to positive outcomes in terms of increased traffic or competition (Oum et al., 1996; Hanlon, 2007; Pitfield, 2007).

*Corresponding author. Tel.: +1-514-572-7367.

E-mail address: khalil.alhandawi@mail.mcgill.ca

Theoretical and empirical studies have affirmed that parallel partnerships (i.e., alliances between airlines that compete on the same routes) are anti-competitive and lead to negative market consolidations while complementary partnerships (i.e., alliances between airlines that do not compete on the same routes) are pro-competitive (Oum et al., 2004; Bilotkach, 2019). However, some studies have suggested that this hypothesis does not always hold true and parallel partnerships can yield benefits to consumers even on the overlapping parts of the joint network due to increased volumes and the economies of traffic density (Brueckner and Whalen, 2000).

Current theoretical research does not fully describe airline partnerships in the context of antitrust immunity (e.g., Open Skies) and joint ventures which are a necessary condition for such partnerships and are often contingent on the approval of government regulators such as the US Department of Justice Antitrust Division. There are a limited number of theoretical and empirical efforts to distinguish between the partnerships that are covered by antitrust immunity and those that are not (Brueckner, 2003; Bilotkach, 2005; Bilotkach and Hüschelrath, 2011). However, these studies focus on specific airline partnership structures such as alliances in isolation and do not fully study the interactions between different partnership types and their combined effects on competition and interline fares. Recent studies have attempted to fill this gap by examining the competitive implications of metal-neutral joint ventures and immunized alliances, yet the results remain mixed and market-specific (Calzaretta et al., 2017).

Furthermore, airline partners often cite the increase in their efficiency as part of their antitrust immunity applications (Oum et al., 2001; Pitfield, 2007). The most commonly used metric for operational efficiency is the load factor defined as the ratio of passenger miles flown to available seat miles (ASMs). It is a measure of how efficiently an airline fills its seats. The load factor is a key metric in the airline industry as it is a measure of how well an airline is utilizing its capacity (Dana and Greenfield, 2019).

Theoretical studies have focused mostly on price effects of airline partnerships. Effects on passenger volumes were automatically realized through the law of demand (i.e., the lower the price, the higher the volume). Some models include economies of traffic density, but they do not explicitly model load factor effects. Such measures are difficult to determine for a regulator due to the proprietary nature of the required data. It is therefore important for regulators to understand the effects of airline partnerships on competition and market consolidation to make informed decisions on the approval of such partnerships (Brueckner, 2001).

Further, a large body of empirical research has focused on US domestic datasets that include at least one flight segment marketed by a US carrier (Bilotkach and Hüschelrath, 2019), as US antitrust laws require airlines to report data on their domestic flights while international flights are not subject to the same reporting requirements. This has led to a lack of empirical studies on international flights and the effects of airline partnerships on international routes (Bilotkach, 2019; Brueckner and Whalen, 2000). By looking at international routes, we can gain a better understanding of the effects of airline partnerships on competition and market consolidation on a global scale (Oum et al., 1996; Bilotkach and Hüschelrath, 2019).

In this work, we focus on a particular airline partnership structure—the airline alliance membership—since it affects the airline network globally and is not specific to any particular domestic market or route. We focus on how alliances can be structured more effectively to truly maximize both competition and the capability of airlines to expand their route networks without leading to negative market consolidations. We first formalize the problem of airline alliance membership as a multi-attribute graph partitioning problem. We then develop a set of metrics to quantify the competition and operational benefits to the airlines and propose a decision making tool for optimizing the airline alliance structure based on flight schedule data which is commonly available to the airlines and regulators through the Official Aviation Guide of the Airways (OAG) dataset. The contributions of this paper are as follows:

- a metric that measures the competitiveness of a flight segment based on the alliance membership of the airlines that operate on that segment;
- a metric that measures the market penetration capability of an airline based on the alliance membership of the airlines that operate on the routes that the airline operates on;
- an optimization problem that maximizes the competitiveness of the routes and the market penetration capability of the airlines simultaneously.
- a set of algorithms to solve this optimization problem.

In Section 2, we provide background information on the data and methods used in this work. In Section 3, we quantify the effects on competition and airline operations in terms of market penetration and then formulate a bi-objective optimization problem using the proposed metrics. In Section 4, we propose optimization algorithms for solving the problem. In Section 5, we present the results of the optimization problem. Section 6 discusses key insights and implications of the results for competition and market consolidation. In Section 7, we provide the conclusion and outline future work.

2. Data and methods

We first describe the data available for this study and the methods used to analyze them. We obtained proprietary data from International Air Transport Association (IATA) that was engineered from the OAG dataset which includes records on passenger bookings and flight schedules (OAG Aviation Worldwide Limited, 2025). We further got information on various airlines and airports from the IATA database. Historical alliance memberships were recovered from public sources and news articles. The data are summarized in Table S.I.

For this study we examine the supply side of the airline industry. We use the ASMs as a measure of supply. The ASMs are a measure of the total number of seats available for sale on a flight. It is calculated by multiplying the number of seats on the aircraft by the number of miles flown. We attempt to develop decision making tools for optimizing the airline alliance structure based on flight schedule data which is commonly available to the airlines and regulators through the OAG dataset.

The data is used to construct a multi-attribute graph of the airport network with airports as nodes $i \in \mathcal{V}$, edges as the flight segments between airports $(u, v) \in \mathcal{E}$, the airlines as the edge attribute $\tau \in \mathcal{T}$ and ASMs being the weight associated with each airline $w_\tau[u, v]$ for all $(u, v) \in \mathcal{E}$ and for all $\tau \in \mathcal{T}$. Such an approach allows us to compactly represent the airline network and the competition between the airlines on all the routes in the network. The graph associated with each airline \mathcal{G}_τ corresponds to its network. The graph \mathcal{G} is the union of all the airline graphs \mathcal{G}_τ .

We show a subgraph of the commercial aviation network for three major middle-eastern airlines in Figure 1. The graph represents the network of airlines and the routes they operate.

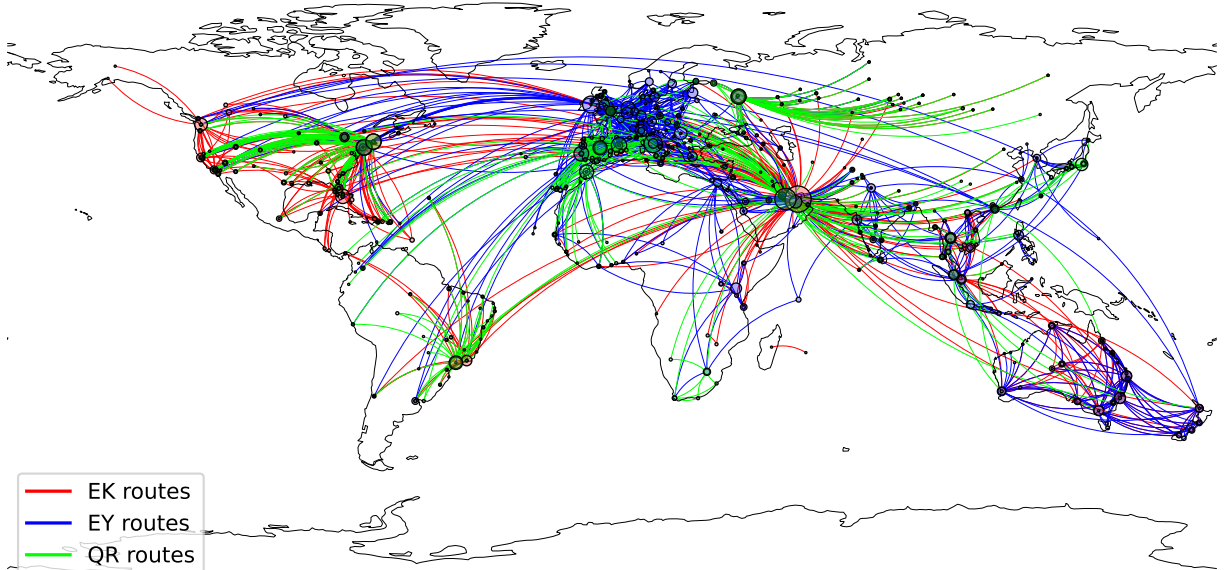


Figure 1: Graph of the IATA network for three major middle-eastern airlines.

Each airline given by an attribute τ can be assigned to an alliance α_k based on the alliance membership data, assuming we have K alliances denoted $\alpha_1, \dots, \alpha_K$. In the following section we define the metrics that govern the competition and the operational benefits to the airlines.

3. Optimization problem formulation

3.1. Competition index calculation

We use the multi-attribute graph of the airport network to calculate, for any segment (u, v) , a metric $h_{u,v}$ representing its competitiveness. This metric, based on the Herfindahl-Hirschman Index (HHI) (Waldman and Jensen, 2012), is estimated as

$$h_{u,v} = \sum_{k=1}^K p(\alpha_k | (u, v))^2 \quad \forall (u, v) \in \mathcal{E}, \forall k = 1, \dots, K, \quad (1)$$

where $p(\alpha_k | (u, v))$ is the conditional probability of observing airline alliance α_k on segment (u, v) . This probability can be estimated using the observed market share of alliance α_k on segment (u, v) given by

$$p(\alpha_k | (u, v)) = \frac{\sum_{\tau \in \mathcal{T}} x_{\tau,k} \cdot w_{\tau}[u, v]}{\sum_{\tau \in \mathcal{T}} w_{\tau}[u, v]}, \quad (2)$$

where $x_{\tau,k}$ is a binary variable that indicates whether airline τ is a member of alliance α_k :

$$x_{\tau,k} = \begin{cases} 1 & \tau \in \alpha_k, \\ 0 & \tau \notin \alpha_k. \end{cases} \quad (3)$$

We can express the ratio $w_{\tau}[u, v]/\sum_{\tau \in \mathcal{T}} w_{\tau}[u, v]$ in terms of a random variable W that follows the probability mass function (PMF) $\mathcal{P}_{u,v}$ of the airlines on segment (u, v) . We can then rewrite the conditional probability (2) in (1) to obtain

$$h_{u,v} = \sum_{k=1}^K \sum_{\tau \in \mathcal{T}} x_{\tau,k} \cdot P(W = w_{\tau}[u, v])^2 = \sum_{k=1}^K \sum_{\tau \in \mathcal{T}} x_{\tau,k} \cdot \mathcal{P}_{u,v}(\tau)^2. \quad (4)$$

Calculating the mean $h_{u,v}$ for all routes has a cost $\mathcal{O}(|\mathcal{T}| \cdot |\mathcal{E}|)$. Alternatively, we can use a sampling technique to estimate $p(\alpha_k | (u, v))$ and reduce the cost to $\mathcal{O}(|\mathcal{E}|)$ for a very large number of airlines $\tau \in \mathcal{T}$.

We construct a sample set $\mathcal{N}_{u,v}$ of airlines that are present on segment (u, v) by drawing n_{samples} independent samples from the PMF $\mathcal{P}_{u,v}$. We can then estimate the conditional probability $p(\alpha_k | (u, v))$ as

$$\hat{p}(\alpha_k | (u, v)) = \frac{1}{|\mathcal{N}_{u,v}|} \sum_{\tau \in \mathcal{N}_{u,v}} x_{\tau,k}, \quad (5)$$

We then approximate the competition index as

$$\hat{h}_{u,v} = \sum_{k=1}^K \left(\frac{1}{|\mathcal{N}_{u,v}|} \sum_{\tau \in \mathcal{N}_{u,v}} x_{\tau,k} \right)^2. \quad (6)$$

3.1.1. Market penetration capability

We also use the multi-attribute graph for calculating a second metric that represents the market penetration capability (MPC) of the airlines. The MPC is a measure of the ability of an airline to access the ASMs of an alliance. We assume that the MPC of an airline τ is proportional to the probability of observing airline τ on a route of length L starting from airport i and observing a member of airline τ 's alliance $\tau' \in \alpha_k$ along the same route.

$$w_{\tau,i} = \sum_{k=1}^K x_{\tau,k} \cdot p(\tau|i, L) \cdot p(\alpha_k|i, L), \quad (7)$$

These probabilities can be calculated by traversing the graph starting from airport i up to a depth L . We first define the PMF of airport u 's neighbourhood as \mathcal{P}_u . Sampling from the PMF \mathcal{P}_u gives us the next airport v . We also use the previous definition of the segment PMF $\mathcal{P}_{u,v}$ to sample the airline τ on the segment (u, v) . We then calculate the MPC of the airlines recursively as

follows:

$$p(\tau|i, L) = \frac{1}{L} \sum_{v \in \mathcal{N}_i} \left(\mathcal{P}_i(v) \mathcal{P}_{i,v}(\tau) + \mathcal{P}_i(v) \sum_{\tau' \in \mathcal{T}} \mathcal{P}_{i,v}(\tau') \cdot p(\tau|v, L-1) \right), \quad (8)$$

$$p(\alpha_k|i, L) = \frac{1}{L} \sum_{v \in \mathcal{N}_i} \left(\mathcal{P}_i(v) \sum_{\tau \in \mathcal{T}} x_{\tau,k} \cdot \mathcal{P}_{i,v}(\tau) + \mathcal{P}_i(v) \sum_{\tau' \in \mathcal{T}} \mathcal{P}_{i,v}(\tau') \cdot p(\alpha_k|v, L-1) \right), \quad (9)$$

where $p(\alpha_k|i, 0) := 0$ and $p(\tau|i, 0) := 0$ for all $i \in \mathcal{V}$ and $\tau \in \mathcal{T}$. The recursive calculation in Equations (8) and (9) can be done using a dynamic programming approach and can be computationally expensive.

We can use a sampling technique to estimate the MPC. We do this by first launching several unbiased independent random walks from every airport $u \in \mathcal{V}$ in the graph. This results in a 3 dimensional tensor

$$V \in \mathcal{V}^{|\mathcal{V}| \times n_{\text{walks}} \times L},$$

where $V_{i,j,l}$ corresponds to the sampled airports along an independent random walk j of length L . The airport tensor $V_{i,j,l}$ is constructed by sampling the next airport $v_{i,j,l+1}$ from the PMF $\mathcal{P}_{v_{i,j,l}}$ of the current airport $v_{i,j,l}$.

$$v_{i,j,l+1} \sim \mathcal{P}_{v_{i,j,l}},$$

where $\mathcal{P}_{v_{i,j,l}}$ is the probability mass function of all the current segments incident to airport $v_{i,j,l}$. The details of the random walk implementation are given in Algorithm 2.

We can convert the tensor $V_{i,j,l}$ to other 3 dimensional tensors

$$T_{i,j,l} \in \mathcal{T}^{|\mathcal{V}| \times n_{\text{walks}} \times L-1}$$

$$W_{i,j,l} \in \mathbb{R}^{|\mathcal{V}| \times n_{\text{walks}} \times L-1},$$

where $T_{i,j,l}$ corresponds to the airline $\tau \in \mathcal{T}$ along segment $(V_{i,j,l}, V_{i,j,l+1})$, while $W_{i,j,l}$ corresponds to the weight of the airline τ along segment $w_{\tau}[V_{i,j,l}, V_{i,j,l+1}]$.

The airline tensor $T_{i,j,l}$ is calculated by sampling from the probability mass function of the airline weights

$$T_{i,j,l} \sim \mathcal{P}_{v_{i,j,l}, v_{i,j,l+1}}.$$

The corresponding weight matrix is updated with the sampled airline weight $w_{T_{i,j,l}}[v_{i,j,l}, v_{i,j,l+1}]$. The details of this sampler are given in Algorithm 3.

Using the tensors T and W , we may compute the MPC of the alliances by aggregating the weights along the j th dimension if the sampled airlines τ are all part of the same alliance α_k .

$$\hat{p}(\alpha_k|i, L) = \frac{1}{n_{\text{walks}} \cdot L} \sum_{j=1}^{n_{\text{walks}}} \sum_{l=1}^L x_{T_{i,j,l}, k}, \quad (10)$$

We then calculate the total weight of each airline τ along the random walk j . This can be expressed mathematically as follows:

$$\hat{p}(\tau|i, L) = \frac{1}{n_{\text{walks}} \cdot L} \sum_{j=1}^{n_{\text{walks}}} \sum_{l=1}^L \mathbf{1}_\tau(T_{i,j,l}), \quad (11)$$

where $\mathbf{1}$ is the indicator function. We then compute the product of (10) and (11) to compute the total gain to airline τ of joining alliance α_k as follows:

$$\hat{w}_{\tau,i} = \sum_{k=1}^K x_{\tau,k} \cdot \hat{p}(\alpha_k|i, L) \cdot \hat{p}(\tau|i, L), \quad (12)$$

(12) describes the relative benefit to airline τ of joining alliance α_k in terms of the airline's ability to access the alliance's ASMs from airport i .

We take the logarithm of the average of $\hat{w}_{\tau,i}$ over all the root airports $i \in \mathcal{V}$ to estimate the MPC of the airlines. This can be expressed as

$$\hat{w}_\tau = \log \left(\frac{1}{|\mathcal{V}|} \sum_{i \in \mathcal{V}} \hat{w}_{\tau,i} \right). \quad (13)$$

The logarithm is used to scale the MPC of the airlines to a more manageable range since we observed that the MPC values in our dataset approximately follow a log-normal distribution. This places more emphasis on the airlines with lower MPC values.

With these metrics, we can formulate an optimization problem that maximizes the competitiveness of the routes and the MPC of the airlines. This can be formulated as a multiobjective optimization problem as follows:

$$\underset{\{\alpha_1, \alpha_2, \dots, \alpha_K\} \in \mathcal{T}^K}{\text{maximize}} \quad -\frac{\beta}{|\mathcal{E}|} \sum_{(u,v) \in \mathcal{E}} \hat{h}_{u,v} + \frac{\gamma}{|\mathcal{T}|} \sum_{\tau \in \mathcal{T}} \hat{w}_\tau,$$

The objective function can be expressed in terms of the binary variable $x_{\tau,k}$ as follows:

$$\underset{\{\alpha_1, \alpha_2, \dots, \alpha_K\} \in \mathcal{T}^K}{\text{maximize}} \quad -\frac{\beta}{|\mathcal{E}|} \sum_{(u,v) \in \mathcal{E}} \sum_{k=1}^K \left(\frac{1}{|\mathcal{N}_{u,v}|} \sum_{t \in \mathcal{N}_{u,v}} x_{t,k} \right)^2 + \frac{\gamma}{|\mathcal{T}|} \sum_{\tau \in \mathcal{T}} \log \left(\frac{1}{|\mathcal{V}|} \sum_{i \in \mathcal{V}} \frac{\hat{p}(\tau|i, L)}{n_{\text{walks}} \cdot L} \sum_{k=1}^K x_{\tau,k} \sum_{j=1}^{n_{\text{walks}}} \sum_{l=1}^L x_{T_{i,j,l},k} \right), \quad (14)$$

where $\beta \in \mathbb{R}^+$ and $\gamma \in \mathbb{R}^+$ are the weights assigned to the two objectives.

4. Solution algorithms

In this section, we explore a variety of algorithms to solve the alliance partitioning optimization problem formulated in (14). We use two algorithms inspired from solutions to modularity maximization for community detection problems in graph theory (Clauset et al., 2004; Fortunato and Hric, 2016; Aref et al., 2024). The optimization problem (14) bears some resemblance to modularity maximization in the sense that we assign a graph attribute to a community. However, our proposed optimization problem has an objective that is fundamentally different to the modularity and focuses on partitioning multi-attribute graphs rather than the nodes of a single attribute graph.

4.1. Greedy method

We utilize a greedy heuristic method for solving the optimization problem. The greedy method is a simple and efficient algorithm that iteratively selects the best possible solution at each step (Clauset et al., 2004). The greedy method is particularly useful when the optimization problem is computationally expensive. and the objective function is non-convex. The greedy method is guaranteed to find a local optimum, but not necessarily the global optimum.

The naive greedy algorithm for solving the optimization problem is given in Algorithm 1. The algorithm initializes each airline as a separate alliance and then iteratively merges the alliances that result in the highest increase in the objective function. The algorithm terminates when the increase in the objective function is less than a predefined threshold or when the number of alliances is equal to 1.

Algorithm 1 Greedy algorithm for optimal partitioning

```

1: procedure GREEDYPART( $\mathcal{G} = (\mathcal{V}, \mathcal{E}, \mathcal{T})$ ,  $T \in \mathcal{T}^{|\mathcal{V}| \times n_{\text{walks}} \times L}$ ,  $\mathcal{N}_{u,v} \forall (u,v) \in \mathcal{E}, \beta, \gamma$ )
2:   Initialize all airlines as separate alliances
   Let  $\alpha_k$  represent an alliance and  $\tau \in \mathcal{T}$  represent an airline
   Assign each airline  $\tau$  to exactly one alliance  $\alpha_k$  using the following constraint:

$$\sum_{k=1}^K x_{\tau,k} = 1, \quad \forall \tau \in \mathcal{T}$$

3:   Compute  $\hat{p}(\tau|i, L) \forall \tau \in \mathcal{T}, i \in \mathcal{V}$  using (11)
4:   Initialize iteration counter  $m \leftarrow 1, K = |\mathcal{T}|$ 
5:   Calculate the objective  $\bar{f}_0$  using (14)
5:   repeat
6:     for  $p$  in  $\{1, 2, \dots, K\}$  do
7:       for  $q$  in  $\{1, 2, \dots, K\}$  do
8:         Merge alliances  $\alpha_p$  and  $\alpha_q$  to form a new alliance  $\alpha_{K+1}$ 
9:         Calculate the objective  $\bar{f}_{(p,q)} = \beta f_{1,(p,q)} + \gamma f_{2,(p,q)}$  in (14)
         excluding the merged alliances  $\alpha_k \notin \{p, q\}$ 
10:        end for
11:      end for
11:      find the best pair  $(p, q) = \underset{p,q}{\text{argmax}} f_{(p,q)}$ 
12:       $m \leftarrow m + 1, K \leftarrow K - 1$ 
12:      until  $f_m - f_{m-1} \leq 0$  or  $K=1$ 
13:      return partitioning of  $\mathcal{G}$  into alliances  $\{\alpha_1, \alpha_2, \dots, \alpha_K\}$ 
14: end procedure

```

A drawback of the greedy method is that it may get stuck in a local optimum and not find the global optimum. To mitigate this, we can run the greedy algorithm multiple times with different initializations and select the partitioning that gives the highest objective value. The greedy method is computationally efficient and can be used to solve large-scale optimization problems.

Another drawback of the above algorithm is the presences of the nested loops which can lead to a high computational cost $\mathcal{O}(K^3)$ in the worst case where K is the number of alliances. We can use an importance sampling technique to choose the most promising pair of alliances (p, q) to merge at each iteration based on the expected increase in the objective. The expected increase in objective can be calculated as follows:

$$\mathbb{E}[\bar{f}_{(p,q)}] = \bar{f}_p + \bar{f}_q, \quad (15)$$

where \bar{f}_p and \bar{f}_q are given by (14). This heuristic can reduce the computational cost to $\mathcal{O}(K)$ and provide some level of exploration in the search space.

4.2. Mixed integer quadratic program (MIQP) formulation

Solving the optimization problem using a mixed integer programming (MIP) algorithm involves formulating the problem as an integer linear program (ILP) model or MIQP. Gurobi is highly capable of solving large-scale ILP problems efficiently, but setting up the problem correctly is crucial. MIQP problems are more complex and may require more computational resources.

The objective involves maximizing the sum of $h_{u,v}$ and $w_{\tau,i}$. The first and second terms in (14) are a quadratic combination of the binary variables $x_{\tau,k}$ and requires an MIQP approach.

We note that the logarithm in (14) cannot be directly implemented in a quadratic program. Instead, we can use a piecewise linear approximation (PWL) approximation of the logarithm function. This involves introducing additional auxiliary variables and constraints.

We introduce auxiliary variables $y_{\tau,i,k}$ to represent the logarithm of the sum of the MPC of the airlines. We can then write the logarithm as a linear combination of the auxiliary variables:

$$\bar{f} = \frac{\beta}{|\mathcal{E}|} \sum_{(u,v) \in \mathcal{E}} \sum_{k=1}^K \left(\frac{1}{|\mathcal{N}_{u,v}|} \sum_{t \in \mathcal{N}_{u,v}} x_{t,k} \right)^2 - \frac{\gamma}{|\mathcal{T}|} \sum_{\tau \in \mathcal{T}} y_{\tau}, \quad (16)$$

where $\varepsilon \leq y_{\tau} \leq 1$ is the auxiliary variable and ε is a small positive constant.

The auxiliary constraint can be written as follows:

$$y_{\tau} = \log z_{\tau}, \quad (17)$$

where z_{τ} is a continuous variable representing the argument of the logarithmic function inside the objective function. i.e.,

$$\text{let } z_{\tau} = \left(\frac{1}{|\mathcal{V}|} \sum_{i \in \mathcal{V}} \frac{\hat{p}(\tau|i, L)}{n_{\text{walks}} \cdot L} \sum_{k=1}^K x_{\tau,k} \sum_{j=1}^{n_{\text{walks}}} \sum_{l=1}^L x_{T_{i,j,l},k} \right),$$

We approximate the constraint in (17) using a PWL approximation. This involves introducing additional auxiliary variables and constraints to linearize the logarithm function.

$$y_{\tau} = \text{PWL}(z_{\tau}, (\varepsilon, 1), (I_1, I_2, \dots, I_{n_{\text{intervals}}}), (V_1, V_2, \dots, V_{n_{\text{intervals}}})), \quad (18)$$

where PWL denotes the PWL approximation function. Here, $(\varepsilon, 1)$ defines the domain of the approximation, $(I_1, I_2, \dots, I_{n_{\text{intervals}}})$ are the breakpoints of the domain, and $(V_1, V_2, \dots, V_{n_{\text{intervals}}})$ are the corresponding function values at these breakpoints. ε is a small positive constant. The breakpoints and values can be calculated as follows:

$$I_k = \varepsilon + \frac{k-1}{n}(1-\varepsilon), \quad k = 1, 2, \dots, n_{\text{intervals}}, \quad (19)$$

$$V_k = \log(I_k), \quad k = 1, 2, \dots, n_{\text{intervals}}. \quad (20)$$

Furthermore, alliance membership is mutually exclusive. Each airline τ should be in exactly one subset α_k :

$$\sum_{k=1}^K x_{\tau,k} = 1 \quad \forall \tau \in \mathcal{T}. \quad (21)$$

The final optimization problem can be written as follows:

$$\begin{aligned}
 & \underset{x_{\tau,k} \in \{0,1\}}{\text{minimize}} \quad \frac{\beta}{|\mathcal{E}|} \sum_{(u,v) \in \mathcal{E}} \sum_{k=1}^K \left(\frac{1}{|\mathcal{N}_{u,v}|} \sum_{t \in \mathcal{N}_{u,v}} x_{t,k} \right)^2 - \frac{\gamma}{|\mathcal{T}|} \sum_{\tau \in \mathcal{T}} y_{\tau} \\
 & \text{subject to} \quad \sum_{k=1}^K x_{\tau,k} = 1 \quad \forall \tau \in \mathcal{T} \\
 & \quad y_{\tau} = \text{PWL}(z_{\tau}, (\varepsilon, 1), (I_1, I_2, \dots, I_{n_{\text{intervals}}}), (V_1, V_2, \dots, V_{n_{\text{intervals}}})) \\
 & \quad z_{\tau} = \left(\frac{1}{|\mathcal{V}|} \sum_{i \in \mathcal{V}} \frac{\hat{p}(\tau|i, L)}{n_{\text{walks}}} \sum_{k=1}^K x_{\tau,k} \sum_{j=1}^{n_{\text{walks}}} \sum_{l=1}^L x_{T_{i,j,l},k} \right) \\
 & \quad x_{\tau,k} \in \{0, 1\}, \quad y_{\tau} \in (-\infty, 0], \quad z_{\tau} \in (0, 1].
 \end{aligned} \tag{22}$$

The following section explores the effectiveness of the greedy and MIQP algorithms in solving the optimization problem on a toy example and a real-world example in Sections 5.1 and 5.2, respectively.

5. Solution and results

In this section, we demonstrate the effectiveness of the greedy and MIQP algorithms in solving the optimization problem formulated in Section 4.2. We first apply the algorithms to a toy example where the optimal solution can be computed exactly. We then apply the algorithms to a real-world example using the IATA dataset.

5.1. Benchmark problem

To create the toy example, we generate a random graph with 20 airports and 2000 segments. We also generate 6 airlines and randomly assign them to the segments. We then run the greedy and MIQP algorithms on this toy example.

The statistics of the toy example are shown in Table 1.

Table 1: Toy example statistics

Parameter	Value	Description
$ \mathcal{V} $	20	number of airports
$ \mathcal{E} $	2000	number of segments
$ \mathcal{T} $	6	number of airlines

We visualize the graph and the airlines in Figure 2.

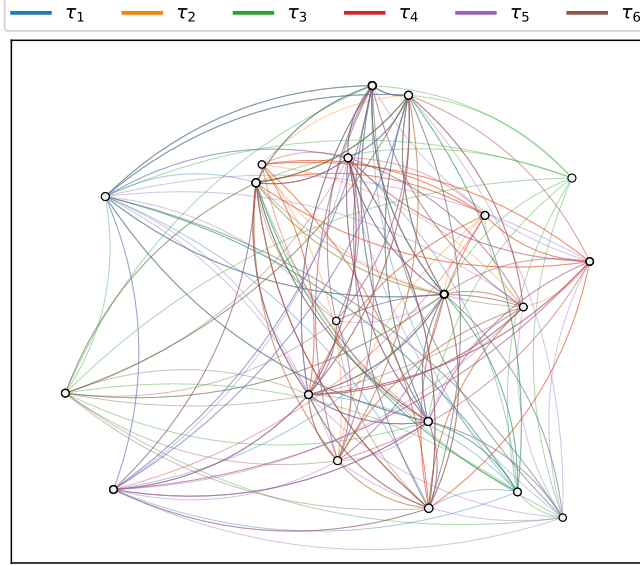


Figure 2: Toy example graph

We first solve the problem exactly by enumerating the possible partitions of the airlines into alliances and evaluating the following objective function without approximating the HHI and MPC terms in (23):

$$\underset{\{\alpha_1, \alpha_2, \dots, \alpha_K\} \in \mathcal{T}^K}{\text{maximize}} \quad -\frac{\beta}{|\mathcal{E}|} \sum_{(u,v) \in \mathcal{E}} h_{u,v} + \frac{\gamma}{|\mathcal{T}|} \sum_{\tau \in \mathcal{T}} w_\tau, \quad (23)$$

The results of the entire enumeration of the solution space are shown in Figure 3b. The best solution out of all the possible enumerations is marked as the oracle solution in Figure 3b and is used as a benchmark to compare the greedy and MIQP algorithms.

Next, we sample the graph using the random walk technique described in Section 3.1.1 and estimate $\hat{h}_{u,v}$ and \hat{w}_τ using Equations (6) and (13) using the settings in Table 2.

Table 2: Optimization problem settings

Parameter	Value	Description
$ \mathcal{N}_{u,v} $	50	number of samples per segment
n_{walks}	50	number of random walks launched per airport
L	2	length of random walk
β	0.7	weight of competition index objective
γ	0.3	weight of MPC objective

We then solve the optimization problem using the greedy algorithm described in Algorithm 1. We set $\beta = 0.7$ and $\gamma = 0.3$ and run the algorithm until termination. We also solve the optimization problem using the MIQP described in Section 4.2.

We also generate $n_{\text{samples}} = 10$ realizations of the randomly sampled variables $t \in \mathcal{N}_{u,v} \forall (u,v) \in \mathcal{E}$ and $T_{i,j,k} \forall i \in \mathcal{V}, j \in \{1, 2, \dots, n_{\text{walks}}\}, k \in \{1, 2, \dots, L\}$ that are used to estimate the HHI and MPC terms in the objective function. We solve the optimization problem using the MIQP and greedy algorithms for each of the 10 realizations to investigate the statistics of the estimated objective function and the sensitivity of the solution to the random sampling.

We compute the final distribution of the objective function values of the MIQP and greedy solutions (without estimation) to compare them against the global maximum obtained by the oracle for all subsequent discussions in this section. The results of this comparison are shown in Figure 3a.

We report the numerical results of the median solution for the oracle, greedy, and MIQP algorithms in Table 3. We note that in some instances, the greedy and MIQP algorithms are able to recover the oracle solution. The MIQP solution has less variance in the objective function values compared to the greedy solution and has a better median objective value.

We report the convergence of the MIQP algorithm for the median solution in Figure 4. The algorithm terminates when an MIP gap of 10^{-6} is reached.

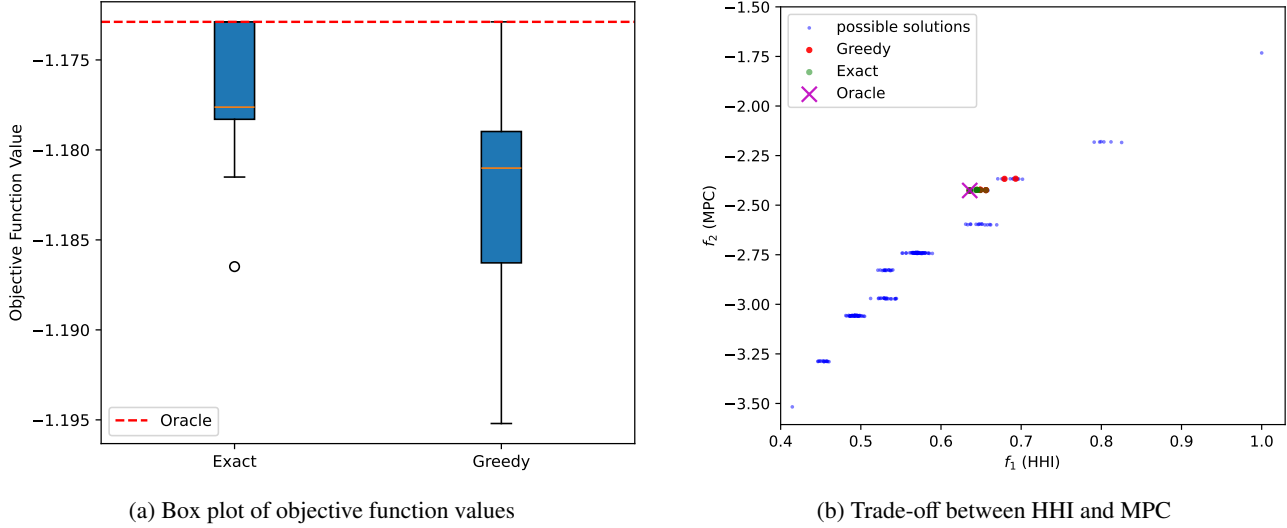


Figure 3: Comparison of the MIQP and greedy algorithms with different realizations of the random sampling. (a) Box plot of the objective function values for the exact and greedy methods. (b) Trade-off between the HHI and MPC in the solution space.

Table 3: Exact method results

Value	Oracle	Greedy (median)	Exact (median)
α_1^*	$\{\tau_1, \tau_3, \tau_4\}$	$\{\tau_1, \tau_4, \tau_6\}$	\emptyset
α_2^*	$\{\tau_2, \tau_5, \tau_6\}$	$\{\tau_2, \tau_3, \tau_5\}$	\emptyset
α_3^*	\emptyset	\emptyset	$\{\tau_1, \tau_5, \tau_6\}$
α_4^*	\emptyset	\emptyset	$\{\tau_2, \tau_3, \tau_4\}$
α_5^*	\emptyset	\emptyset	\emptyset
α_6^*	\emptyset	\emptyset	\emptyset
Objective	-1.173	-1.183	-1.176
HHI	-0.636	-0.638	-0.650
MPC	-2.426	-2.457	-2.427

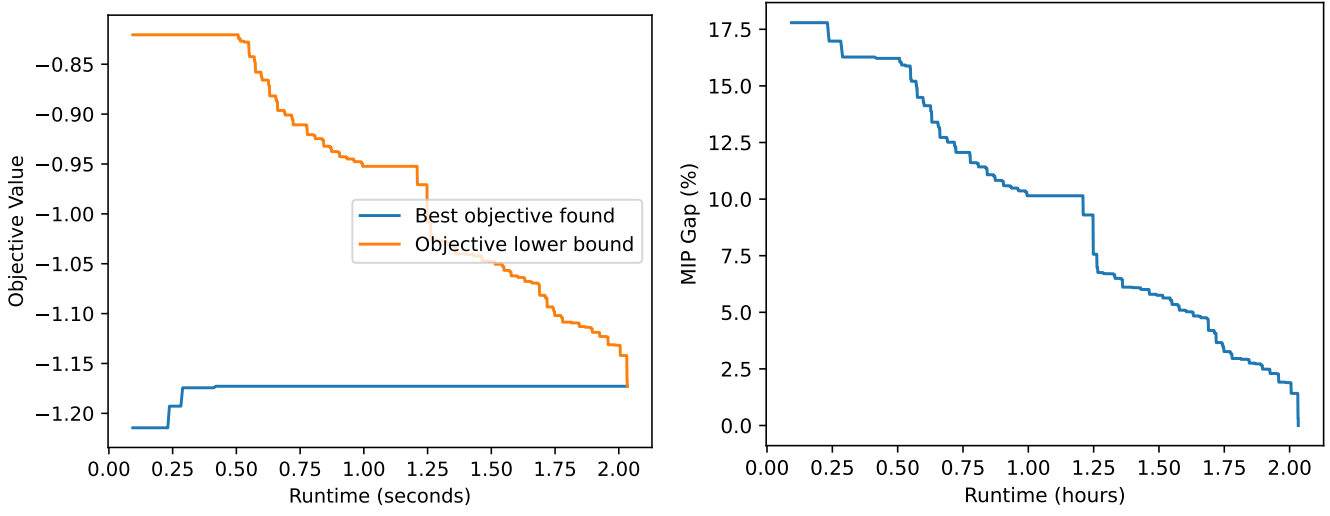


Figure 4: Visualization of optimal partitioning with (a) optimal membership shown and (b) the alliance membership shown.

5.2. Results on IATA network

As described in Section 2, we obtain data from IATA that describes the supply and demand data along different routes in the form of ASMs and passenger revenue miles (RPMs), respectively. The statistics of the IATA network are shown in Table 4.

Table 4: Toy example statistics

Parameter	Value	Description
$ \mathcal{V} $	3680	number of airports
$ \mathcal{E} $	160732	number of segments
$ \mathcal{T} $	580	number of airlines

We solve the optimization problem using the greedy algorithm described in Algorithm 1. We set $\beta = 0.25$ and $\gamma = 0.75$ and run the algorithm until termination. Table 5 below summarizes the optimization problem settings.

Table 5: Optimization problem settings

Parameter	Value	Description
$ \mathcal{N}_{u,v} $	100	number of samples per segment
n_{walks}	20	number of random walks launched per airport
L	3	length of random walk
K	580	number of alliances to be detected

5.3. Greedy optimization results

The greedy algorithm terminates after 365 iterations. This means, that 215 alliances are formed out of a total of 580 airlines.

We construct a secondary graph where the airports are the airlines and the edges are the codeshared ASMs between the airlines. This graph helps us visualize the airline alliances and any partitioning obtained via the algorithms in this paper in the context of codesharing.

We use the Fruchterman-Reingold algorithm to project the airlines into a 2D space and visualize the optimal partitioning in Figure 5. We also show the alliance membership of the airlines in Figure 5b (Fruchterman and Reingold, 1991).

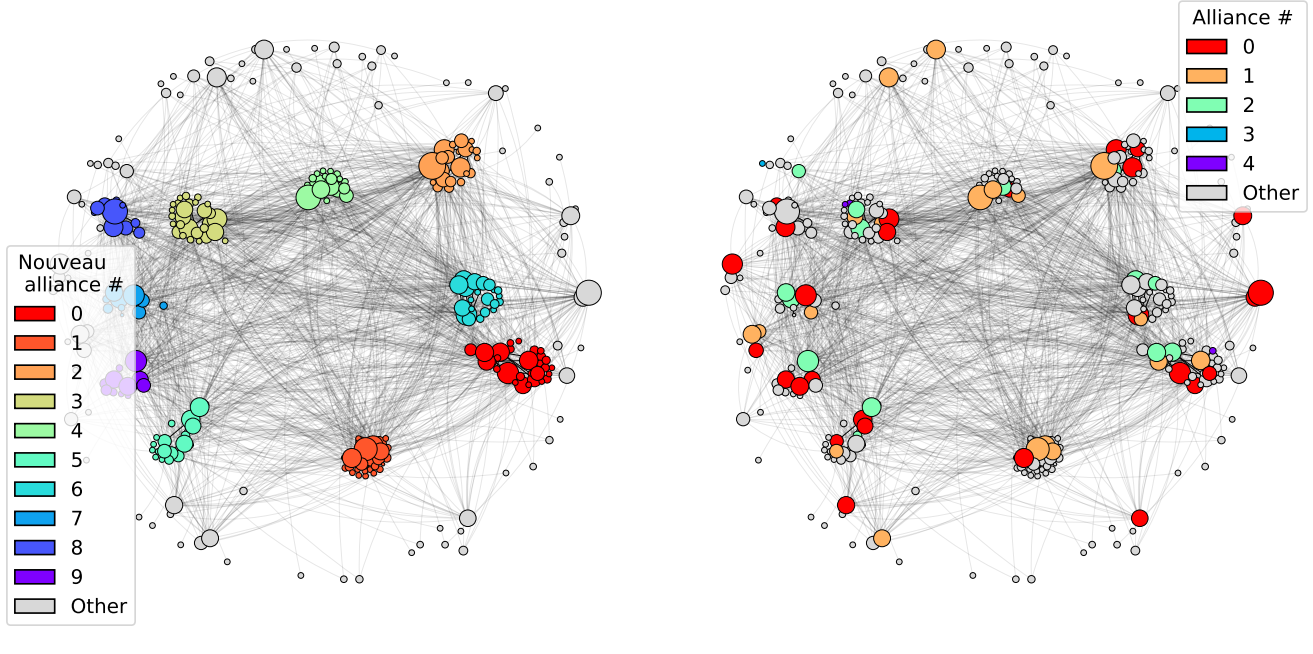


Figure 5: Visualization of optimal partitioning with (a) optimal membership shown and (b) the alliance membership shown.

The algorithmic convergence is shown in Figure 6. The algorithm trades off some competitiveness to increase the MPC of the airlines. The importance of each objective can be adjusted using the weights β and γ .

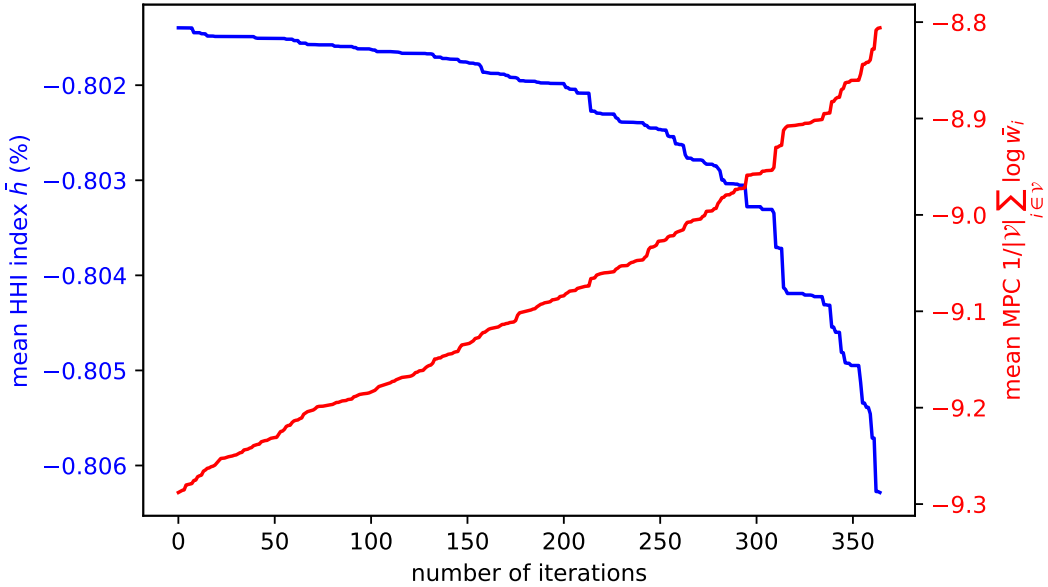


Figure 6: Convergence of the greedy algorithm.

We compute the final objective values using an independent realization of the random walks for a fair comparison with other algorithms.

The value of the MPC term is $1/|\mathcal{V}||\mathcal{T}| \sum_{\tau \in \mathcal{T}} \sum_{i \in \mathcal{V}} \log \hat{w}_{\tau,i} = -8.7856$, i.e., the mean MPC was $e^{-8.7856}$. The value of the HHI index is $\bar{h} = 1/|\mathcal{E}| \sum_{(u,v) \in \mathcal{E}} h_{u,v} = 0.8073$.

5.4. Exact optimization results

We also solve the optimization problem in (22) using a MIQP approach. We use the Gurobi solver with default settings.

Due to memory cost considerations, we reduced the sampling effort to accomodate the quadratic objective terms in memory during optimization. We reduce the number of samples per segment $|\mathcal{N}_{u,v}|$ from 100 to 10, and the number of independent random walks per airport n_{walks} from 20 to 10, and the number of alliances to be detected K from 580 to 30.

Table 6 below describes the problem parameter settings for the MIQP approach.

Table 6: Optimization problem settings for the MIQP approach

Parameter	Value	Description
$ \mathcal{N}_{u,v} $	10	number of samples per segment
n_{walks}	10	number of random walks launched per airport
L	3	length of random walk
K	30	number of alliances to be detected

Table 7 shows the model statistics for the MIQP.

Table 7: Model statistics for the MIQP

Statistic	Value
Total number of binary variables	1,080
Total number of continuous variables	17,370
Total number of constraints	579
Total number of general constraints (for PWL approximation)	540
Total number of quadratic non-zero coefficients	2,050,380

We use the following Gurobi MIQP settings shown in Table 8.

Table 8: Optimization problem settings for the MIQP approach

Parameter	Value	Description
TimeLimit	72,000	Time limit in seconds for running the MIP solver
NodefileStart	0.5	When to start writing branch and bound node data to disk
SoftMemLimit	54GB	Terminate the solver if this memory limit is reached
MIPGap	0.001	Terminate the solver if the gap is within 0.1%
SolutionLimit	∞	Limits the number of feasible MIP solutions found
Heuristics	0.15	Controls the aggressiveness of the heuristics used
MIPFocus	1 (feasibility)	Focus on finding new feasible solutions over proving solution optimality or improving optimality
Cuts	0	Disable all cuts
Presolve	0	Disable presolve
ScaleFlag	1	Enable scaling of the problem
Method	1	Use the dual simplex method
FeasibilityTol	1e-2	Feasibility tolerance for the solver
IntFeasTol	1e-3	Integer feasibility tolerance for the solver

For evaluation purposes, we compare the objective function values of the partitioning obtained via the MIQP on the same independant realization of the random walks for a fair comparison. i.e., we compute the terms in (22) using the MIQP and greedy solutions $x_{\tau,k}^{\text{MIQP}}$ and $x_{\tau,k}^{\text{greedy}}$ using an independent realization of random walks obtained with the settings in Table 5.

The final objective value for the MPC term is $1/|\mathcal{V}||\mathcal{T}| \sum_{\tau \in \mathcal{T}} \sum_{i \in \mathcal{V}} \log \hat{w}_{\tau,i} = -8.9016$, i.e., the mean MPC was $e^{-8.9016}$. The HHI index value is $\bar{h} = 1/|\mathcal{E}| \sum_{(u,v) \in \mathcal{E}} \hat{h}_{u,v} = 0.8021$.

This shows that the MIQP solution places more emphasis on maintainig the competitiveness of the partitioning while improving the MPC relative to the greedy optimization results in Section 5.3.

The airline graph is projected on 2D Cartesian space for visualization using the partitioning obtained by the MIQP in Figure 7a. The airline alliances are shown in Figure 7b.

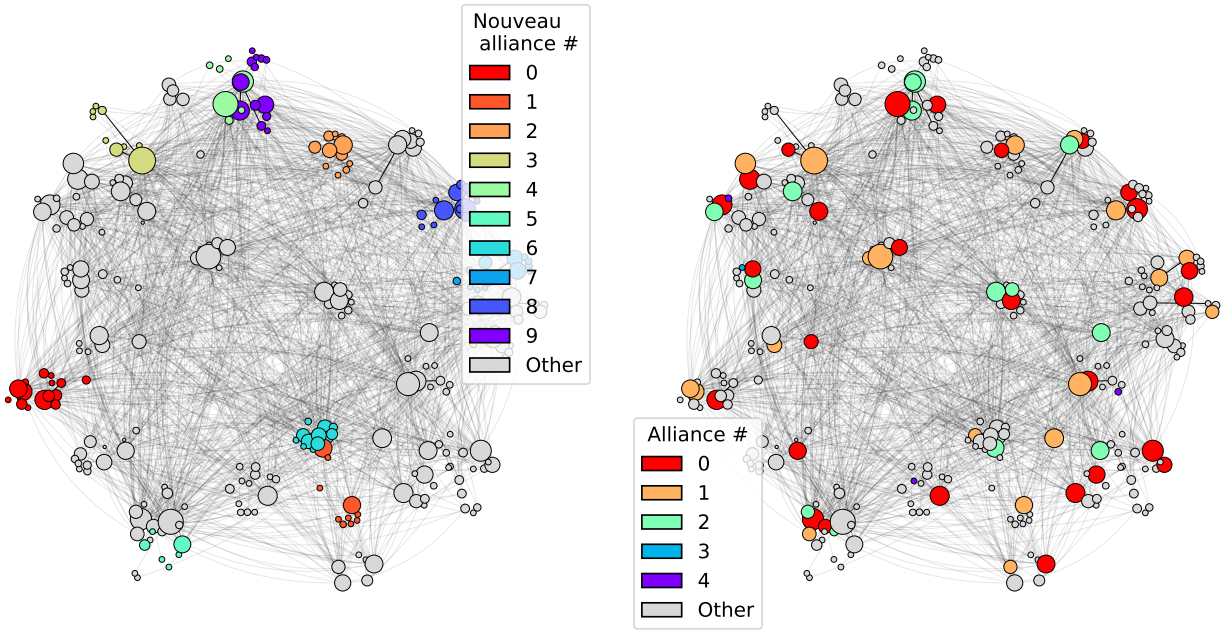


Figure 7: Visualization of optimal partitioning with (a) optimal membership shown and (b) the alliance membership shown.

Finally, we repeat all the computations performed in Sections 5.3 and 5.4 for $\beta = 0.75$ and $\gamma = 0.25$, i.e., placing more emphasis on the HHI term in the objective function. The results are shown in Table 10 for comparison and are discussed in the following section.

A summary of the results of these evaluations is shown in Table 9

In Figure 8, we show the distribution of the competition index $h_{u,v}$ and the MPC $\hat{w}_{\tau,i}$ for the partitioning obtained by each of the algorithms reported in Table 9. We show the results for both $\beta = 0.25$ and $\gamma = 0.75$ and $\beta = 0.75$ and $\gamma = 0.25$.

Table 9: Results of the greedy and MIQP optimization methods relative to the alliance partitioning

Method	HHI term (%)	MPC term	objective f
$\beta = 0.25, \gamma = 0.75$			
Existing alliances	80.22	-9.2974	-7.1736
Greedy algorithm	80.73	-8.7856	-6.791
MIQP	80.21	-8.9016	-6.8767
$\beta = 0.75, \gamma = 0.25$			
Existing alliances	80.22	-9.2974	-2.926
Greedy algorithm	80.16	-9.0497	-2.8636
MIQP	80.19	-8.829	-2.8087

We note that the range of possible values is $[0, 1]$ and $[-\infty, 0]$ for the HHI and the logarithm of MPC, respectively. The lower the HHI, the more competitive the segment is, while the higher the MPC, the more efficient the airline is by virtue of its ability to access new markets.

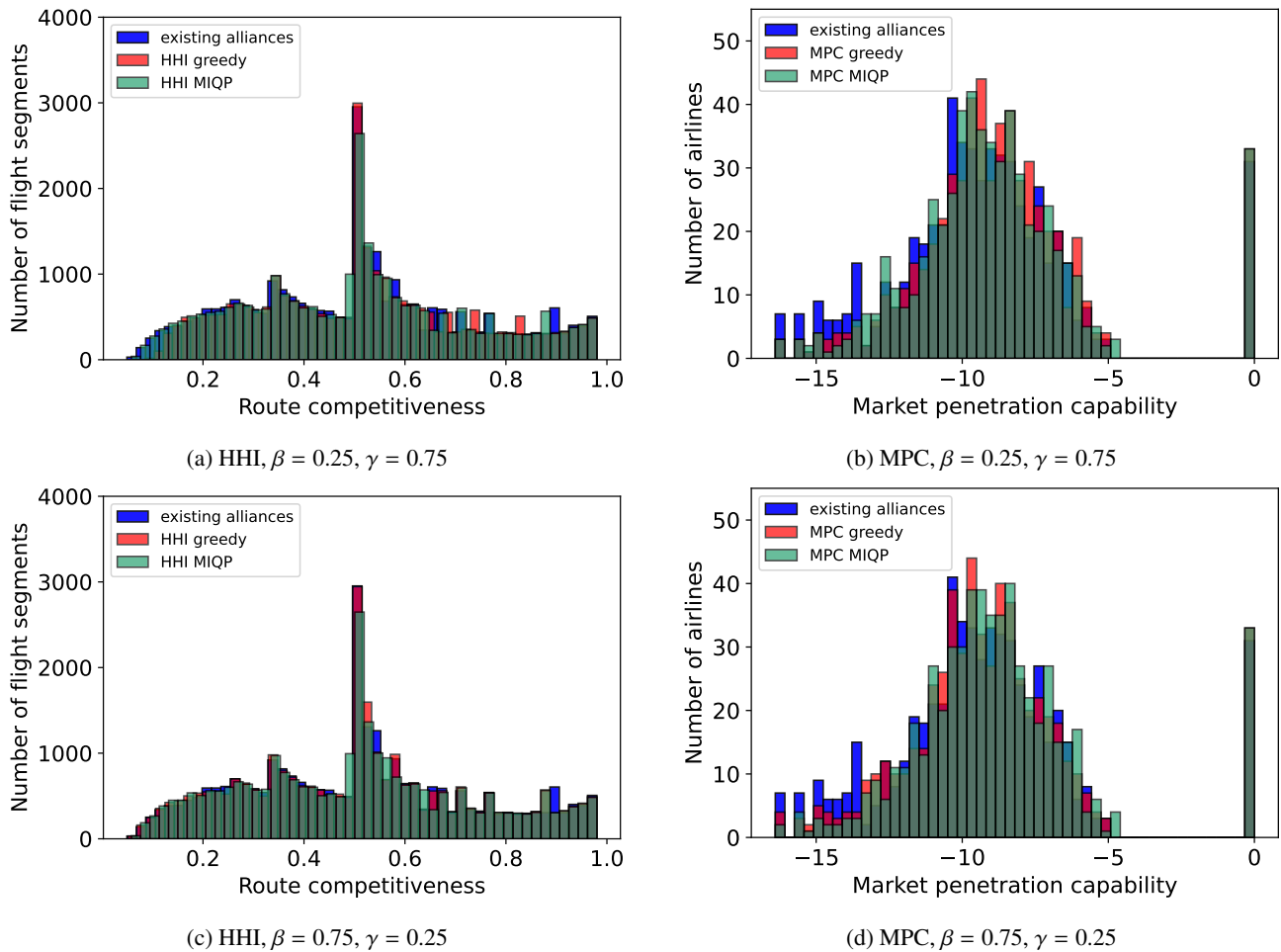


Figure 8: Distribution of the HHI ($h_{u,v} \forall (u,v) \in \mathcal{E}$) and MPC ($1/|\mathcal{V}| \sum_{i \in \mathcal{V}} \log \bar{w}_\tau \forall \tau \in \mathcal{T}, i \in \mathcal{V}$) for the greedy algorithm and the MIQP solution relative to the existing alliances.

We also examine the cumulative mass function (CMF) of the MPC to determine the benefit of the partitioning to the airlines relative to the existing alliances. The CMF of the MPC is shown in Figure 9. It can be seen that the MIQP solution improves the MPC of the airlines when less weight is placed on the MPC term in the objective function. The MIQP algorithm generally performs better when the overall objective function value is small due to the smaller weight placed on the MPC term.

To make a fair comparison between the different algorithms, 10 statistically independent optimization runs are performed with each algorithm using 10 different realizations of the random walks. The solutions are then evaluated using another 10 realizations of the random walks to estimate the objective function values. These results are discussed in detail in the following section.

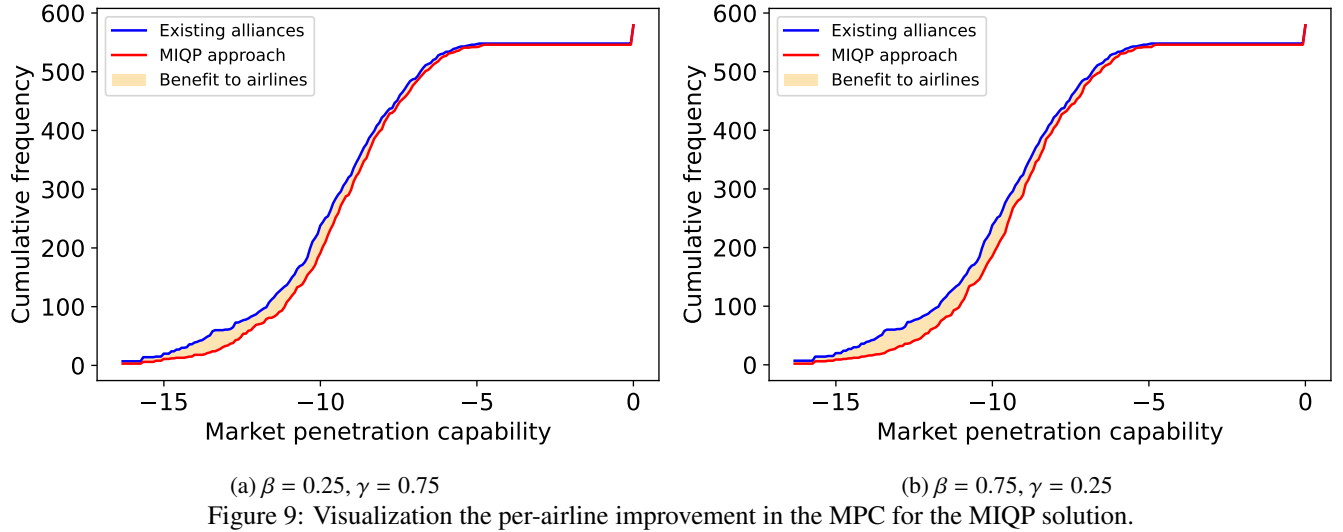


Figure 9: Visualization the per-airline improvement in the MPC for the MIQP solution.

6. Discussion and comparison

The following table summarizes the performance of the partitioning obtained by the existing alliances, the greedy optimization method, and the MIQP optimization method. We conduct 10 statistically independent runs of the greedy and MIQP optimization methods to investigate the sensitivity of the solution to the random sampling.

The boxplot in Figure 10 shows the distribution of the objective function components for the greedy and MIQP solutions. All partitions (including alliances) exhibit comparable variance values for the HHI and MPC terms. All algorithms (MIQP and greedy method) result in an improvement of both objective terms relative to the alliances. The best improvement in the HHI terms was found by the greedy method when setting the HHI weight to $\beta = 0.75$.

Table 10: Results of the greedy and MIQP optimization algorithms relative to the alliance partitioning

Method	HHI (%)		logMPC		objective f	
	mean	std. σ	mean	std. σ	mean	std. σ
$\beta = 0.25, \gamma = 0.75$						
Existing alliances	80.216	5e-05	-9.25616	0.08296	-7.14266	0.06222
Greedy algorithm	80.705	5e-05	-8.80688	0.08082	-6.80692	0.06061
MIQP	80.205	6e-05	-8.90454	0.08038	-6.87892	0.06028
$\beta = 0.75, \gamma = 0.25$						
Existing alliances	80.216	5e-05	-9.25616	0.08296	-2.91566	0.02073
Greedy algorithm	80.159	5e-05	-9.07647	0.08151	-2.87031	0.02036
MIQP	80.208	6e-05	-8.84455	0.07989	-2.8127	0.01996

We can see that both algorithms yield an improvement in the MPC and HHI relative to the existing alliances. The MIQP solution is less sensitive to changes in the weighting coefficients β and γ as compared to the greedy method. This could be due to the large MIP gaps encountered during the solution process and insufficient exploration of the branch and bound tree.

However, the MIQP solution performed reliably and consistently on smaller graphs such as those in Section 5.1 suggesting that such approaches are more suitable for smaller graphs. The greedy algorithm is more suitable for larger graphs due to its lower memory requirements and faster convergence. This observation is consistent with the results and observations in the context of community detection and modularity maximization (Aref et al., 2023).

7. Conclusion

In this paper, we proposed a framework for optimizing airline alliance partnerships while balancing negative externalities such as market concentration and reduced competition with potential improvements to the airlines' operational efficiency in terms of market penetration. We formulated the problem as a multi-objective optimization problem and proposed a greedy algorithm and a MIQP approach to solve the problem. We evaluated the performance of the algorithms on a toy example and a real-world airline network obtained from IATA data.

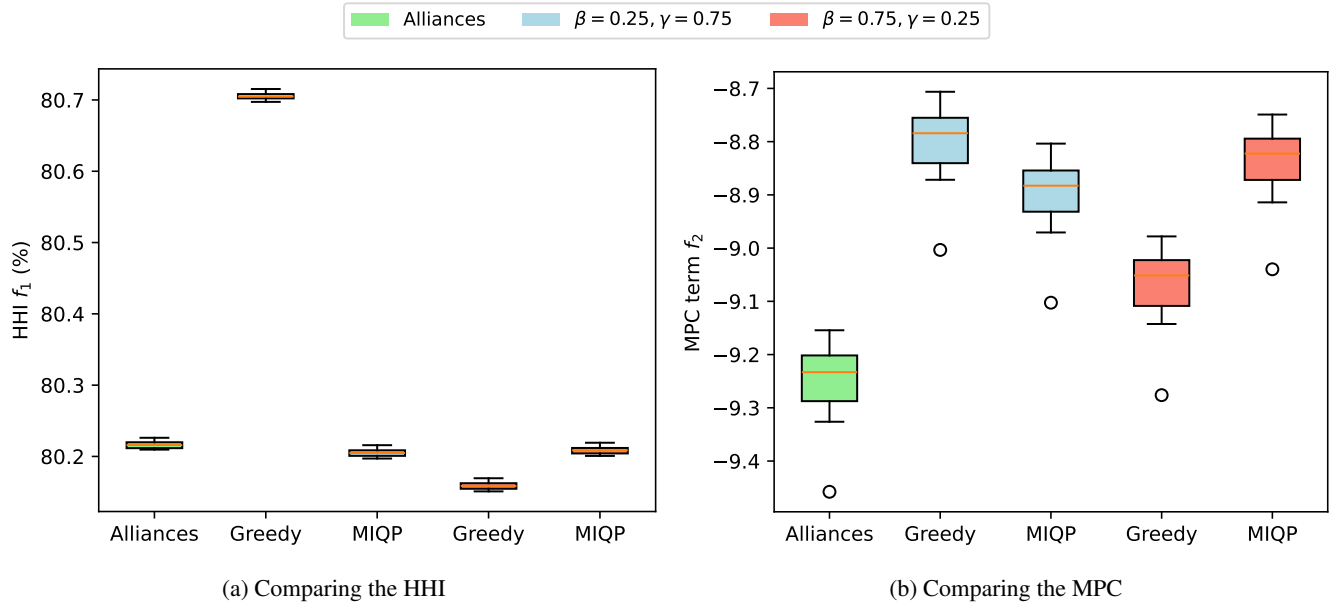


Figure 10: Visualization of the distribution of the estimated HHI and MPC for the greedy and MIQP solutions using 10 independent runs and 10 independent realizations of the random walks.

Our approaches yielded promising improvements to the global aviation markets compared to the existing alliances as baselines. This structured mathematical optimization approach was able to find a good balance between the network's HHI and market penetration capability (MPC) for a given alliance structure.

This nuanced approach can highlight the need for innovative alliance strategies and/or regulatory adjustments to ensure that the benefits of alliances are realized both for the airlines and their passengers, fostering a competitive but also cooperative aviation market (Pitfield, 2007).

Acknowledgements

The authors wish to acknowledge the support of the National Science and Engineering Research Council of Canada (NSERC) through the Postdoctoral Fellowship program and the Discovery Grants program. The authors also wish to thank IATA for providing the data used in this study.

References

Aref, S., Mostajabdeh, M., Chheda, H., 2023. Heuristic modularity maximization algorithms for community detection rarely return an optimal partition or anything similar, in: Mikyška, J., de Matalier, C., Paszynski, M., Krzhizhanovskaya, V.V., Dongarra, J.J., Sloot, P.M. (Eds.), Computational Science – ICCS 2023, Springer Nature Switzerland, Cham. pp. 612–626.

Aref, S., Mostajabdeh, M., Chheda, H., 2024. Bayan algorithm: Detecting communities in networks through exact and approximate optimization of modularity. *Physical Review E* 110, 044315. doi:[10.1103/PhysRevE.110.044315](https://doi.org/10.1103/PhysRevE.110.044315).

Bilotkach, V., 2005. Price competition between international airline alliances. *Journal of Transport Economics and Policy* 39, 167–189. doi:[10.2139/ssrn.607449](https://doi.org/10.2139/ssrn.607449).

Bilotkach, V., 2019. Airline partnerships, antitrust immunity, and joint ventures: What we know and what i think we would like to know. *Review of Industrial Organization* 54, 37–60. doi:[10.1007/s11151-018-9636-x](https://doi.org/10.1007/s11151-018-9636-x).

Bilotkach, V., Hüschelrath, K., 2011. Antitrust immunity for airline alliances. *Journal of Competition Law and Economics* 7, 335–380. doi:[10.1093/joclec/nhq029](https://doi.org/10.1093/joclec/nhq029).

Bilotkach, V., Hüschelrath, K., 2019. Balancing competition and cooperation: Evidence from transatlantic airline markets. *Transportation Research Part A: Policy and Practice* 120, 1–16. doi:[10.1016/j.tra.2018.12.008](https://doi.org/10.1016/j.tra.2018.12.008).

Brueckner, J.K., 2001. The economics of international codesharing: an analysis of airline alliances. *International Journal of Industrial Organization* 19, 1475–1498. doi:[10.1016/S0167-7187\(00\)00068-0](https://doi.org/10.1016/S0167-7187(00)00068-0).

Brueckner, J.K., 2003. International airfares in the age of alliances: The effects of codesharing and antitrust immunity. *Review of Economics and Statistics* 85, 105–118. doi:[10.1162/003465303762687749](https://doi.org/10.1162/003465303762687749).

Brueckner, J.K., Whalen, W.T., 2000. The price effects of international airline alliances. *Journal of Law and Economics* 43, 503–545. doi:[10.1086/467464](https://doi.org/10.1086/467464).

Calzaretta, Robert J., J., Eilat, Y., Israel, M.A., 2017. Competitive effects of international airline cooperation. *Journal of Competition Law & Economics* 13, 501–548. doi:[10.1093/joclec/nhx016](https://doi.org/10.1093/joclec/nhx016).

Clauset, A., Newman, M.E., Moore, C., 2004. Finding community structure in very large networks. *Physical Review E - Statistical Physics, Plasmas, Fluids, and Related Interdisciplinary Topics* 70, 6. doi:[10.1103/PhysRevE.70.066111](https://doi.org/10.1103/PhysRevE.70.066111).

Dana, J.D.J., Greenfield, D.J., 2019. The impact of passenger mix on load factors in the airline industry. *Review of Industrial Organization* 54, 111–127. doi:[10.1007/s11151-018-9631-2](https://doi.org/10.1007/s11151-018-9631-2).

Fortunato, S., Hric, D., 2016. Community detection in networks: A user guide. *Physics Reports* 659, 1–44. doi:[10.1016/j.physrep.2016.09.002](https://doi.org/10.1016/j.physrep.2016.09.002).

Fruchterman, T.M., Reingold, E.M., 1991. Graph drawing by force-directed placement. *Software: Practice and Experience* 21, 1129–1164.

Hanlon, P., 2007. *Global Airlines: Competition in a Transnational Industry*. 3rd ed., Butterworth-Heinemann, Oxford, UK.

OAG Aviation Worldwide Limited, 2025. Official aviation guide. URL: <https://www.oag.com>.

Oum, T.H., Park, J.H., Kim, K., Yu, C., 2004. The effect of horizontal alliances on firm productivity and profitability: evidence from the global airline industry. *Journal of Business Research* 57, 844–853. doi:[10.1016/S0148-2963\(02\)00484-8](https://doi.org/10.1016/S0148-2963(02)00484-8).

Oum, T.H., Park, J.H., Zhang, A., 1996. The effects of airline codesharing agreements on firm conduct and international air fares. *Journal of Transport Economics and Policy* 30, 187–202.

Oum, T.H., Yu, C., Zhang, A., 2001. Global airline alliances: international regulatory issues. *Journal of Air Transport Management* 7, 57–62. doi:[10.1016/S0969-6997\(00\)00034-X](https://doi.org/10.1016/S0969-6997(00)00034-X). proceedings of the Hamburg Aviation Conference 2000.

Pitfield, D.E., 2007. The impact on traffic, market shares and concentration of airline alliances on selected European-US routes. *Journal of Air Transport Management* 13, 192–202. doi:[10.1016/j.jairtraman.2007.03.002](https://doi.org/10.1016/j.jairtraman.2007.03.002).

Waldman, D.E., Jensen, E.J., 2012. *Industrial Organization: Theory and Practice*. 4 ed., Pearson.

Supplemental Material: Background

S.I. Details of the air travel dataset

Table S.I provides a summary of the data used for the purposes of this research. It is derived from OAG and complemented by data provided by IATA.

Table S.I: Summary of available data from industrial problem solving workshop

Data Field	Dataset	sources			
		OAG	proprietary (IATA)	Public	Derived
Name (IATA, ICAO designation)	Airport	✓			
latitude/longitude		✓			
Region		✓			
Name (IATA, ICAO designation)	Airline	✓			
Startup/Shutdown/merger dates		✓			
Region		✓			
Airline (IATA, ICAO designation)	IOSA registry		✓		
Date of Audit closure			✓		
Registration expiry			✓		
Demand (RPM)	Passenger	✓			
Reported + Est. Pax		✓			
Operating/Marketing flight numbers		✓			
Flight number		✓			
Origin/Destination code		✓			
International/Domestic flight					✓
Flight numbers	Schedules	✓			
Operating/Marketing flight		✓			
Origin/Destination code		✓			
Number of stops		✓			
Stopping airports		✓			
Supply (ASM)		✓			
International/Domestic flight					✓
COVID years (March 2020 - May 2021)	misc.		✓	✓	
Airline alliance membership			✓	✓	

S.II. Random walk implementation

We use random walks to sample flight paths on the airport graph $\mathcal{G}(\mathcal{V}, \mathcal{E})$. We begin by launching multiple independent random walks of length L for every $i \in \mathcal{V}$ in our graph. The airport i is denoted as the root airport for the random walk. During every step, the random walker checks the weights $\text{weight}(v_i, v_j)$ of the segments associated with the current airport v_i , where $i = [1, 2, \dots, L - 1]$ and $v_j \in \mathcal{N}(v_i)$ is a neighboring airport.

The tensors of the random walk described in Section 3.1.1 are populated by the random walker.

$$V \in \mathcal{V}^{|\mathcal{V}| \times n_{\text{walks}} \times L}, \quad (\text{S.1})$$

where $V_{i,j,k}$ corresponds to the sampled airports along an independent random walk j of length L .

The implementation of the random walker is given by Algorithm 2.

Algorithm 2 Weighted Random Walks (from all sources)

```

1: procedure WEIGHTEDRANDOMWALKS( $\mathcal{P}_i \forall i \in \mathcal{V}, L, n_{\text{walks}}$ )
2:   for each  $i \in \mathcal{V}$  do
3:     for  $j = 1$  to  $n_{\text{walks}}$  do
4:        $V_{i,j,1} \leftarrow i$ 
5:       for  $k = 1$  to  $L$  do
6:         sample  $V_{i,j,k+1} \sim \mathcal{P}_{V_{i,j,k}}(\cdot)$  ▷ neighbor PMF at current airport
7:       end for
8:     end for
9:   end for
10:  return  $V$ 
11: end procedure

```

A conditional samples is used to populate the tensors of the airlines and weights of the segments traversed by the random walker in Algorithm 2.

$$T_{i,j,k} \in \mathcal{T}^{|\mathcal{V}| \times n_{\text{walks}} \times L-1} \quad (\text{S.2})$$

$$W_{i,j,k} \in \mathbb{R}^{|\mathcal{V}| \times n_{\text{walks}} \times L-1}, \quad (\text{S.3})$$

where, $T_{i,j,k}$ and $W_{i,j,k}$ correspond to the sampled airlines $\tau \in \mathcal{T}$ and weight $w \in \mathbb{R}$, respectively, at each step of the random walk. The conditional sampler is given by Algorithm 3.

Algorithm 3 Conditional Sampling of Edge Attributes and Weights

```

1: procedure CONDITIONALSAMPLING( $\mathcal{P}_{u,v} \forall u, v \in \mathcal{E}, V, L$ )
2:   for each  $i \in \mathcal{V}$  do
3:     for  $j = 1$  to  $n_{\text{walks}}$  do
4:       for  $k = 1$  to  $L - 1$  do
5:          $u \leftarrow V_{i,j,k}, v \leftarrow V_{i,j,k+1}$ 
6:         sample  $T_{i,j,k} \sim \mathcal{P}_{u,v}(\cdot)$  ▷ airline on segment  $(u, v)$ 
7:          $W_{i,j,k} \leftarrow w_{T_{i,j,k}}[u, v]$  ▷ airline-specific segment weight
8:       end for
9:     end for
10:   end for
11:   return  $T, W$ 
12: end procedure

```

We can easily parallelize the to outer loops i and j in Algorithm 2 and i, j, k to accelerate the computation of the tensors V , T , and W .